Thermal Profile of a Lanthanum Hexaboride Heaterless Hollow Cathode

IEPC-2017-291

Presented at the 35th International Electric Propulsion Conference
Georgia Institute of Technology • Atlanta, Georgia • USA
October 8 – 12, 2017

Alexander Daykin-Iliopoulos[1], Igor Golosnoy[2] and Steve Gabriel[3]
University of Southampton, SO17 1BJ, United Kingdom

Abstract: Higher power cathodes are increasingly utilizing LaB_6 emitters due to their increased emission current density capabilities over barium oxide emitters, however, these emitters require higher operating temperatures which poses a significant challenge to maintain heater reliability. Hence, there is ongoing development of heaterless hollow cathodes that allow for potentially higher reliability through design simplicity of removing the heater component, and in addition, there is potential savings in mass, volume, ignition time and power. In this study a LaB_6 heaterless hollow cathode with imbedded high temperature thermocouple instrumentation demonstrated reliably operation in diode mode from 5-8 A at xenon flow rates of 0.2-1.75 sccm. The temperature profile of the emitter is characterized through ignition, which lasts up to 50 seconds. In addition, pyrometer measurements in an open keeper configuration have shown the emitter surface temperature to be significantly lower than that predicted by the Richardson equation for LaB_6 emitter, perhaps indicating a strong influence of the surface chemistry.

Nomenclature

P_1	=	pressure down steam of orifice [Torr]
P_2	=	pressure up steam of orifice [Torr]
Q	=	mass flow rate [sccm]
T	=	temperature [K]
l	=	orifice length [cm]
d	=	orifice diameter [cm]
p	=	pressure [Pa]
$\dot{m}$	=	mass flow rate [kg·s^{-1}]
A	=	orifice cross-sectional area [m^2]
T	=	temperature [K]
R	=	gas constant [J·mol^{-1}·K^{-1}]
γ_c	=	heat capacity ratio
T_i	=	indicative temperature [k]
T_t	=	true temperature [k]
ζ	=	optical transmittance
n	=	molar mass [kg·mol^{-1}]
λ	=	wavelength [μm]

[1] PhD Student, Tony Davies High Voltage Laboratory, Alexander.Daykin-Iliopoulos@soton.ac.uk.
[2] Associate Professor, Tony Davies High Voltage Laboratory, ig@ecs.soton.ac.uk.
[3] Professor, Tony Davies High Voltage Laboratory, sbg2@soton.ac.uk.

ε = emissivity
J = emission current [A·cm^{-2}]
D_0 = coefficient in Richardson-Dushman equation [A·cm^{-2}K^{-2}]
e = electron charge [C]
$\emptyset_{wf}$ = work function [eV]
k = Boltzmann's constant [J·K^{-1}]

I.Introduction

The development of high powered hollow cathodes is of importance to meet the demand of increasingly powerful Gridded Ion engines and Hall Effect thrusters[1]. Higher power cathodes are increasingly utilizing lanthanum hexaboride (LaB_6) emitters, due to the high-density emission, lifetime and improved handling capabilities over traditional barium oxide emitters. However, LaB_6 cathodes theoretically operate at temperatures ~400 K higher than Barium Oxide cathodes, which operate around 1500 K, dependent on emission current. This poses greater challenges for raising the emitter temperature to these higher emissive temperatures in order to enable cathode ignition.

The ohmic heater component commonly used to raise the emitter temperature for thermionic emission, has inherent reliability issues from thermal fatigue caused by the thermal cycling with large temperature variations. A heaterless hollow cathode allows for potentially higher reliability through design simplicity of removing the heater component. In addition, there are multiple other benefits including reduction in ignition time from minutes to seconds due to direct emitter heating through ion bombardment, and, significantly reduced manufacturing costs due to heater removal as well as the removal of the heater power supply.

In heaterless hollow cathodes (HHC) the emitter heating is driven by a discharge between the keeper and the emitter. This method of ignition comprises of three main stages: breakdown, heating, and nominal operation. Successful operation at a given stage does not always result in transition to a further stage[2]. However, due to the lack of thermionic emission during heaterless ignition, high voltages (~900 V) and high flow rates (>20 sccm) are required to heaterless ignite conventional designs[3]. Most commonly in heaterless cathodes the keeper orifice is reduced[4] to increase the pressure in the emitter-keeper region lowering the ignition voltage and mass flow rates required. However, this can have drawbacks, namely reduced election extraction efficiency, resulting in relatively high anodic voltages and increase keeper erosion.

In order to facilitate the design of HHCs with reasonable starting characteristics (< 0.5 kV, < 20 sccm) and comparable performance characteristics with conventional HCs, the emitter temperature profile through ignition is measured. Accordingly, a HHC instrumented with thermocouples along the emitter is developed to characterize the emitter thermal profile through heaterless ignition as well as during steady state operation.

As such, the study aids the understanding of the plasma heat flux throughout ignition and nominal operation, as well as providing data for thermal model validations in future work. In addition, the voltage, current and mass flow rate characteristics are determined with the corresponding emitter profile. Finally, the future testing of the HHC with anodic discharges and corresponding parametric investigations are outlined.

II.Thermal characterization of LaB_6 heaterless ignition

A. Heaterless hollow cathode

A second generation laboratory model lanthanum hexaboride heaterless hollow cathode (see Figure 1 & Figure 3) has been utilized for this study. This laboratory model was developed to investigate the operating characteristics of heaterless hollow cathodes, as such it is a modular design which allows for relatively easy instrumentation. Overall, the HHC has similar attributes in terms of design and material selection to an engineering model, although sufficient thermal and structural optimization is required for such development.

The heaterless hollow cathode consists of a stainless steel mounting flange, which can attaches to the chamber mount via mounting bolts that are electrically isolated with ceramic alumina corner washers. The cathode propellant line protrudes from the rear of the mounting flange, and connects to a 1/8 inch Swagelok fitting, with a ceramic isolator upstream, that connects to the main propellant line of the chamber. A molybdenum cathode tube 70 mm in length with a 4.9 mm inner diameter is secured to the mounting flange. The lanthanum hexaboride emitter with an inner diameter of 2 mm, outer diameter of 4.5 mm, and a length of 20 mm is inserted into the end of the molybdenum cathode. A fine graphite sleeve is used to electrically connect, yet mechanically separate the LaB_6 emitter from the refectory tube, due

to the known issues of boron diffusion[1]. A casing supports the multilayered tantalum thermal shield placed downstream of the cathode tube, which reduces the radiative thermal losses of the HHC during operation.

Figure 1. Mounted second-generation LaB_6 heaterless hollow cathode

The enclosed keeper is made from POCO EDM-3 graphite. The orifice diameter of the keeper used in this study is 0.25 mm, which is intentionally constructed as small as reasonably possible despite the resultant electron extraction difficulties. This is in anticipation of a future study of the keeper orifice diameter, at which point the orifice will be systematically expanded and tested with an additional anode discharge to quantitatively assess these electron extraction difficulties. Typically the keeper orifice diameter is in the order of two or three times that of the cathode orifice diameter, for conventional cathodes as the keeper both aids ignition stabilization as well as protect from high energy ion bombardment[5].

The cathode pressure is predominantly dependent on the constrictive office size and mass flow rate. As the keeper orifice is the most constrictive orifice in the flow stream in this HHC, Goebel's commonly used internal cathode pressure equations [5] can be used to calculate the cathode-keeper pressure for the:

$$P_1 = \left(P_2^2 + \frac{0.78 Q \zeta T_r l}{d^4}\right)^{0.5} \quad , \zeta = 2.3 * 10^{-4} T_r^{\,0.71+\frac{0.29}{T_r}} \tag{1.1}$$

where P_1 is the pressure in Torr, P_2 is the pressure downstream of the choked orifice in Torr, d is the orifice diameter in cm, l is the orifice length in cm, $Tr = \frac{T}{289.7}$, where T is temperature in Kelvin and finally Q is mass flow rate in sccm. Goebel has found this to be 10-20% of the actual measured pressures though as the author explains the equation is not strictly valid in some HC locations, especially in the case of short orifices. Thus, by assuming the flow is choked at the keeper orifice, the choked flow mass flow rate equation[6] can also been used for comparison:

$$\dot{m} = \frac{pA}{\sqrt{T}} \sqrt{\frac{\gamma_c}{R_s} \left(\frac{2}{\gamma_c + 1}\right)^{\frac{\gamma_c+1}{(\gamma_c-1)}}} \tag{2.1}$$

when rearranged it gives,

$$p = \left(\frac{A}{\dot{m}\sqrt{T}} \sqrt{\frac{\gamma_c}{R_s} \left(\frac{2}{\gamma_c + 1}\right)^{\frac{\gamma_c+1}{(\gamma_c-1)}}} \right)^{-1} \tag{2.2}$$

Where, $\dot{m}$ is mass flow rate in kg/s, A is the orifice cross-sectional area in m^2, γ_c is the heat capacity ratio, for Xe at 300 K it is taken to be 1.66, $Rs = R/n$, R is the gas constant taken to be 8.314 $J \cdot mol^{-1} \cdot K^{-1}$, n is molar mass for xenon

taken to be 131.29 kg·mol^{-1}, T is the temperature at the orifice in K, and p is the pressure in Pa. Figure 2 shows both Eq. 1.1 and Eq. 2.2 plotted, for mass flow rate of 5 sccm.

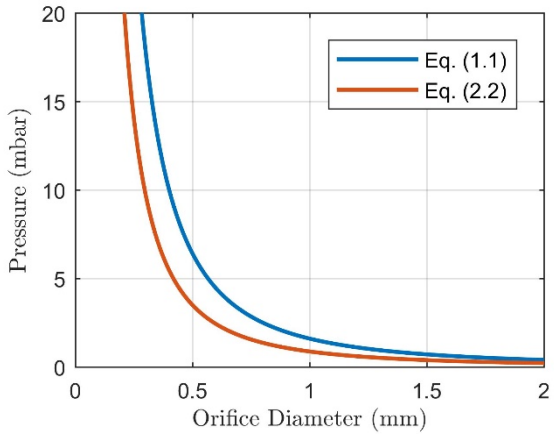

Figure 2. Keeper orifice sizing, T=300 K, l=1.5 mm, $\dot{m}_{Xe} = 5$ sccm

B. Instrumentation

Due to the high operating temperatures of hollow cathodes, standard Type K thermocouples that can withstand ~1100°C would be insufficient for this purpose, thus Type C Thermocouples (Tungsten 5%, Rhenium 95% - Tungsten 26% Rhenium 74%) that can operate up to 2325°C [7] were utilised, short-term exposures are also possible to 2760°C, though such ultra-high temperature operation is not required for this application. The accuracy of the thermocouple is ±4.5°C up to 450°C beyond which it is ±1% reading.

As there is known issues with boron diffusion reaction with the thermocouples[8], the thermocouples where placed in the emitter sleeve, mechanically isolating the thermocouples from the emitter, while also being less intrusive to the emitter. The thermocouples are sheathed in dual bore alumina tubing. The alumni tubing network, which can be withstand up to 1900°C, insulates the thermocouples wires throughout the cathode as can be seen in Figure 3.

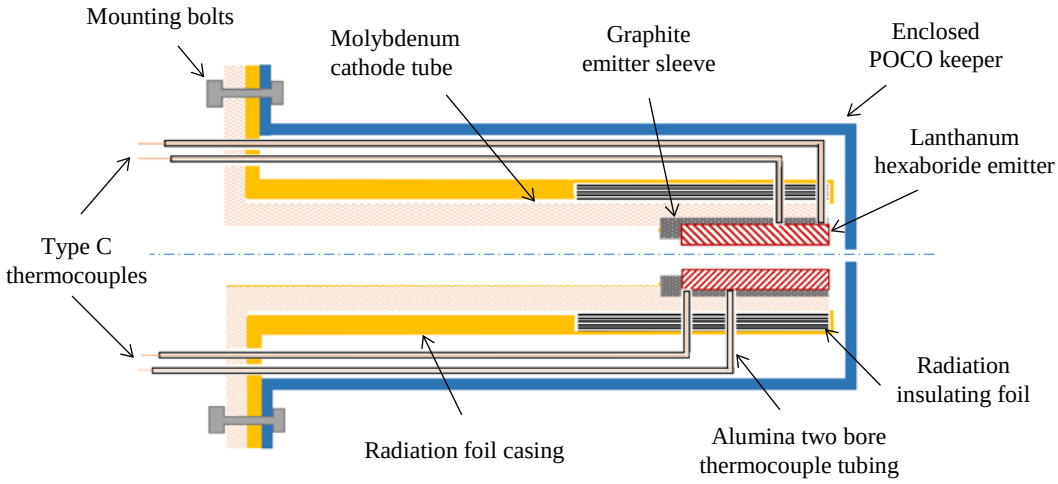

Figure 3. HHC, with integrated thermocouple instrumentation

There are four thermocouple measurement locations to determine the emitter thermal profile throughout operation (see Figure 3 & Figure 4). The thermocouples are inserted perpendicular to the cylindrical cathode surface, through the thermal shielding, cathode tube and partially through the emitter sleeve. The thermocouples are oriented at equal

azimuthal and radial increments along the emitter, such that each thermocouple is at 45° azimuthally. The respective axial distances as a ratio of the total emitter length, l, from the emitter tip is: $4l/5$, $3l/5$, $2l/5$ and $l/5$.

To minimize the thermal impact, as the thermocouple is an intrusive instrument, the two bore alumina tube is as small as reasonably possible, with an outer diameter 1.3 mm, and 0.3 mm inner diameters bore, each thermocouple wire diameter is 0.127 mm. For the thermocouples to make good thermal contact with the cathode, mechanical pressure is applied to the thermocouple in the direction of the emitter and set in place by sealing the alumina tube at the base of the cathode with, Zirconia ceramic paste[9].

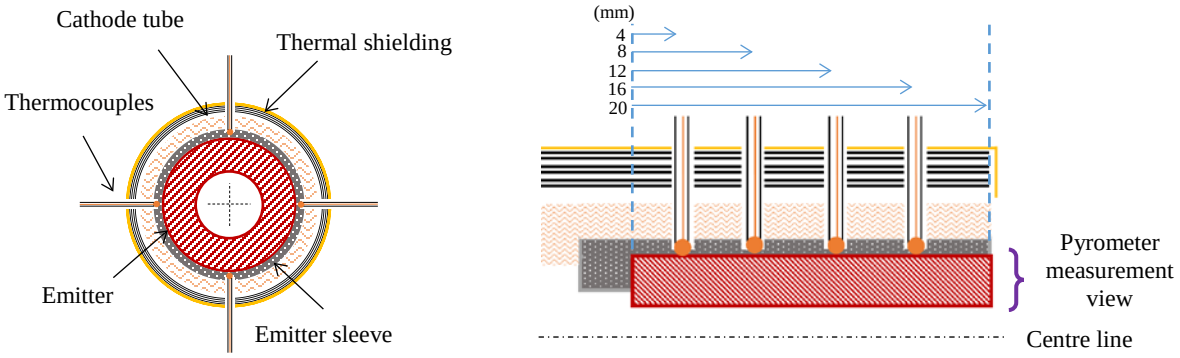

Figure 4. Thermal instrumentation measurement locations

For axillary temperature measurement of the emitter surface a Spectrodyne Inc. DFP 2000 portable disappearing filament optical pyrometer is utilized. This pyrometer operates at a wavelength, λ, of 0.65 μm, and has a total range of 760°C to 4200°C. The pyrometer range operated in this study maintained an accuracy above 0.3% of reading $\pm$ 1 digit. For accurate pyrometer measurements corrections are needed for the emissivity, ε, of the target at the measured wavelength. In addition, adjustment to the emissivity is required to take account of the chamber widow optical transmittance, ζ, at λ, such that the effective emissivity $\varepsilon_{\lambda_{e,\zeta}} = \varepsilon_\lambda \, \zeta_\lambda$. For the borosilicate glass window of the chamber the optical transmittance is taken to be $\zeta_\lambda = 0.91$ and the LaB_6 emissivity[10] is:

$$\varepsilon_\lambda = 1.2144 - 2.467 * 10^{-4} T_i \tag{3.1}$$

So to correct from the indicative temperature, T_i in kelvin, measured by the pyrometer at λ to the true surface temperature T_t in kelvin[11]:

$$T_t = \frac{1}{\left(\frac{1}{T_i}\right) + \left(\frac{log\ \varepsilon_{\lambda_{e,\zeta}}}{9613}\right)} \tag{3.2}$$

C. Electrical and control circuitry

The electrical system of the heaterless hollow cathode system can been seen in Figure 5. An EA-PS 9750-12, 750V, 12A power supply, supplies the HHC electrical control system (ECS) to ignite the HHC. The keeper-cathode voltage is measured by a Pico Technology TA042 differential voltage probe, which is logged via the Tektronix DPO3034 Digital Oscilloscope, 300MHz, 2.5 Gsps. All four thermocouples are connected and logged by a Pico Tech TC-08 logger, which is connected to the PC system through an isolator.

All live data from the subsystems including the, voltage probe, oscilloscope, power supply and TC logger are transmitted and recorded by the PC LabView control system. With heaterless ignition, a separate power supply for the heating stage is not required due to the plasma heating the emitter from cold. The current setup is for a keeper only discharge which ignites the HHC, for operation in which the discharge is extracted to an anode, an additional power supply is required, which applies potential to anode in respect to the cathode, as with conventional cathodes.

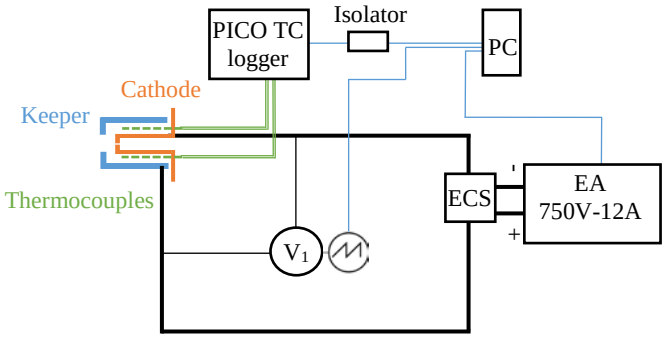

Figure 5. HHC with integrated instrumentation, electrical and control circuitry

D. Facility setup

Due to the enclosed geometries of the HHC[3], namely the enclosed keeper, it is beneficial to investigate the discharge in an open geometry experimental set-up to allow more detailed diagnostics. Thus, TDHVL-VC3 vacuum facility (see Figure 6) was utilized for this testing due to the backfilling capability allowing for both open keeper and enclosed keeper setups.

TDHVL-VC3 facility consists of a 35 cm diameter spherical stainless steel vacuum chamber, with numerus CF16, CF40 & CF100 flanges, allowing for easy instrumentation access and mounting. An Edwards RV5 pump vacuum pump reduces the chamber base pressure to ~ 9×10-3 mbar at which point an Edwards Next 400D turbo pump controlled via PC interface, lowers and maintains a base pressure of ~ 3×10-7 mbar prior to operation. A gate valve is connected between the turbo pump and the vacuum chamber to allow isolation of the turbo pump from the chamber so backfilling is possible. The chamber pressure was measured by a Pfeiffer Balzers IKR-020 Penning gauge and a TPR 010 Pirani gauge, displayed on a TPG-300 vacuum gauge controller, corrections factors are implemented for xenon. An additional Applied Vacuum Barometric 1-50 mbar dial gauge was utilized for determining the cathode line pressure.

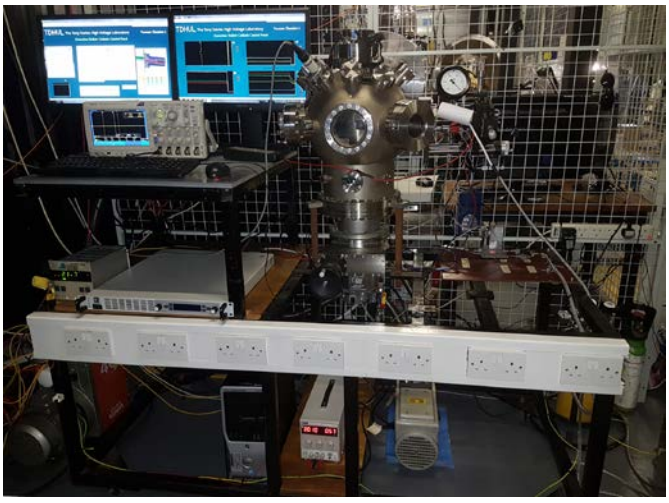

Figure 6. TDHVL-VC3 facility setup

The propellant system is controlled by a Bronkhurst EL-FLOW mass flow controller (MFCs) with 0-20 sccm flow rate range, which is supplied by a N4.8 Xenon gas cylinder used for the experiments in this study. The mass flow rate controller is connected to a PC and controlled via the LABView software. An additional manual bypass was in place for large pressure increases. The pipeline from the MFCs to the chamber has a manual valve on the chamber side to isolate the propellant system from the chamber, which is left open during pump down operation.

E. Test configurations

The testing in this study was done in two configurations (1) backfilled with external keeper and (2) enclosed keeper with gas flow (see Figure 7):

(1) The backfilled system with an external keeper is diagnostically beneficial to investigate the keeper discharge as the open discharge allows for visual inspection of the plasma and pyrometer access to the emitter.

When the system has reached base pressure (~2×10-7 mbar) to remove impurities, the propellant system valve is closed, and this pipe section to the chamber is backfilled with by the MFCs or with the manual bypass dependent on the required chamber pressure. Once the pipeline is backfilled the chamber gate valve is closed isolating the turbo pump from the chamber. As soon as the pump is isolated the propellant system valve is opened rapidly backfilling to the required pressure. This process is to minimize outgassing of from the chamber system.

In this mode the keeper is connected separately on the opposite side of the chamber to the cathode system. A manual XYZ position manipulator that manipulates the cathode system, with the integrated diagnostics. The manipulator allows for cathode XY alignment with an accuracy of $\pm$ 0.05 mm, so that it is concentric with the keeper, and the keeper-cathode electrode separation, d_{k-c}, can be varied with a movement accuracy of $\pm$ 0.01 mm. The d_{k-c} is zeroed by reducing the gap with the manipulator until a conductive path is made between the cathode and keeper, then from that point the required separation is set.

(2) The enclosed keeper with gas flow system is the normal mode of operation of the HHC. The keeper is enclosed on the cathode as shown in Figure 3, with the open keeper removed from the chamber. In this mode of operation the gate valve is not used, instead the flow system, which is connected to the rear of the cathode, is used to pressurize the keeper-cathode internal system. Once the mass flow is operated, the cathode line pressure is indicated on the barometric dial gauge. Typically the chamber back pressure throughout testing remains below 4×10^{-4} mbar.

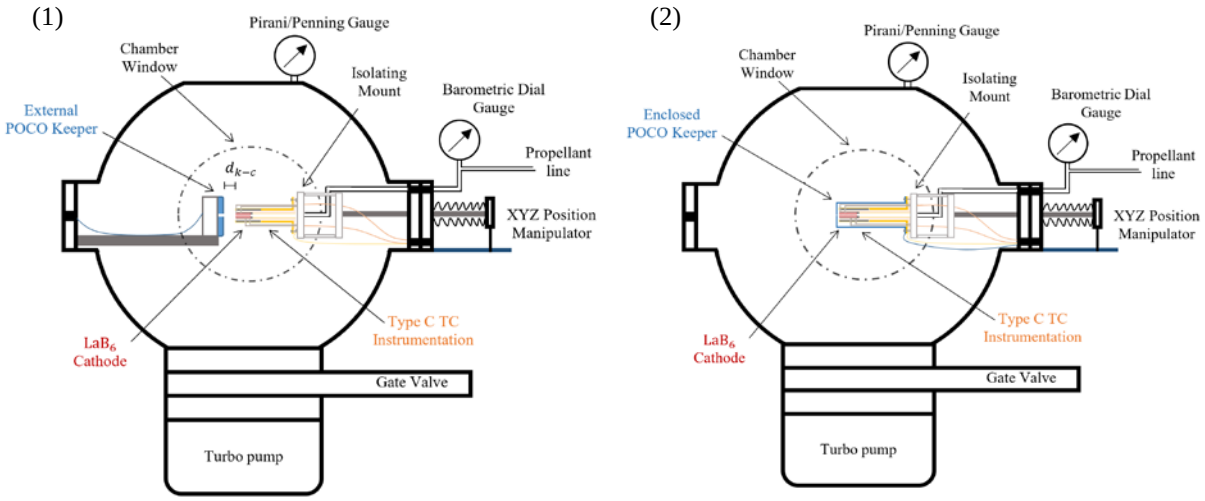

Figure 7. Experimental setups – (1) backfilled with external keeper configuration, (2) enclosed keeper with gas flow

III.Results and discussion

For this studies experimental campaign, the HHC was operated in diode mode, in which there is only a keeper current and no anode current. As mentioned the open configuration was used to allow pyrometer measurements of the emitter surface. The main difference found in operation in the open keeper configuration and enclosed configuration was the improved ignition stability and reliability with the enclosed configuration. This influence is perhaps predominantly due to the enclosed keepers geometric differences, such as the keeper increased size, and that the keeper is surrounding the cathode reducing the possible election wall/chamber losses that occur in the open geometry configuration. The data trends reported in this study have been found to be reproducible over various tests, though further data gathering is required to for accurate statistical analysis of the data, such as mean and standard deviation plotting. In addition, the conjoining lines of the data points shown are only for easier identification of the data sets.

A. External keeper – steady state operation

In Figure 8, the pyrometer temperature measurements of the emitter tip, T_p are displayed along with the thermocouple measurements from T_1 to T_4, see Figure 4 for measurement locations. T_2 detached during this testing, and hence is not shown in this plot.

Throughout the overall experimental campaign and as shown in Figure 8 the highest temperatures where typically recorded at the tip of the emitter, for T_p this was around 1270°C to 1460°C and for T_1 this was around 830°C to 1060°C from 1 to 4 A respectively. As can be seen the thermocouples are significantly lower, ~400°C, than that of the pyrometer readings. Each thermal measurement, including the pyrometer, is in equal axial movements of 4 mm along the emitter (see Figure 4), and the typical axial temperature gradient along the emitter recorded by the thermocouples is 22 °C/mm, hence the axially gradient only accounts for ~90°C from T_1 to T_p. Therefore, it is likely that the reason for this large temperature disparity is significantly due to the radial positioning of the thermocouple, which is exacerbated by high thermal contact resistance of the emitter-sleeve contact. Although there is large disparity in the absolute temperature of the pyrometer and thermocouples, the $T_1 - T_p$ relation followed very similar trends throughout testing, hence considered sufficient for preliminary trend analysis of the emitter thermal profile, as reported in this study.

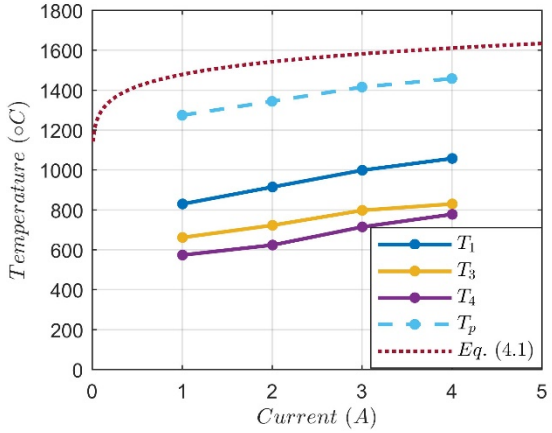

Figure 8. Thermal profile comparison, 1st configuration, 9 mbar back pressure, $\dot{m} = 5$ A

The measured temperature data has also been compared with the theoretical temperature calculated by the modified Richardson equation[5]:

$$J = D_0 T^2 e^{-\frac{e\emptyset_{wf}}{kT}} \tag{4.1}$$

where $\emptyset_{wf}$ is the material work function, D_0 is a temperature-modified coefficient to the Richardson-Dushman, in A/cm^{2}K^2, T is temperature in K, and J is the current density in A/cm^2. The emission is assumed uniform across the

emitter surface which appears conservative as there is a high thermal gradient, and also the electron current is assumed equal to the total current. The work function was taken to be 2.67 eV, and $D_0 = 29$ A/cm^{2}K^2,[12] though there are several different work functions published, from 2.67 to 2.91[10, 12, 13] due to the corresponding D_0 being varied and use of the non-corrected coefficient to the Richardson-Dushman[14] the authors are actually only within 25% of one another[15].

The Richardson's emission is shown in Figure 8 as the fine-dashed line, and it can be seen that it is higher than the measured temperatures. The temperature difference is 200°C to 150°C from 1 to 4 A. One main reason for this difference may be due to the Schottky effect, where the electric field enhancement effectively lowers the work function. However, it would be required to lower the work function of up to 0.34 to 0.24 eV to match the pyrometer temperatures measured from 1 to 4 A respectively. Lower temperatures then theoretically calculated have also been observed for conventionally ignited cathodes, Polk[8] postulates that this is due to the lanthanum being ionized and recycled back to the emitter surface due to its lower ionization potential, resulting in a lanthanum rich emitter, LaB_4 and hence a reduction in the material work function. Further investigation of this process is intended.

B. Enclosed keeper – ignition characteristics

Figure 9 shows a characteristic HHC ignition profile from room temperature, ~17°C from 0 to 5 A. After the 1.75 sccm is set, which corresponds to a cold cathode pressure of 5.5 mbar, a potential is applied between the cathode-keeper electrodes, causing the gas to electrical breakdown around 350 V. With breakdown there is the formation of the gaseous discharge with a power of around 150 to 240 W, heating the emitter primarily through ion bombardment. This heating phase lasts around 35 seconds dependent on the emitter heat flux. After sufficient emitter heating, substantial thermionic emittance occurs and a transition to nominal operation where the discharge voltage drops to around 30 V at 5 A, transition can take up to 15 seconds. In nominal operation mode the emitter temperature is also sustained by ion bombardment.

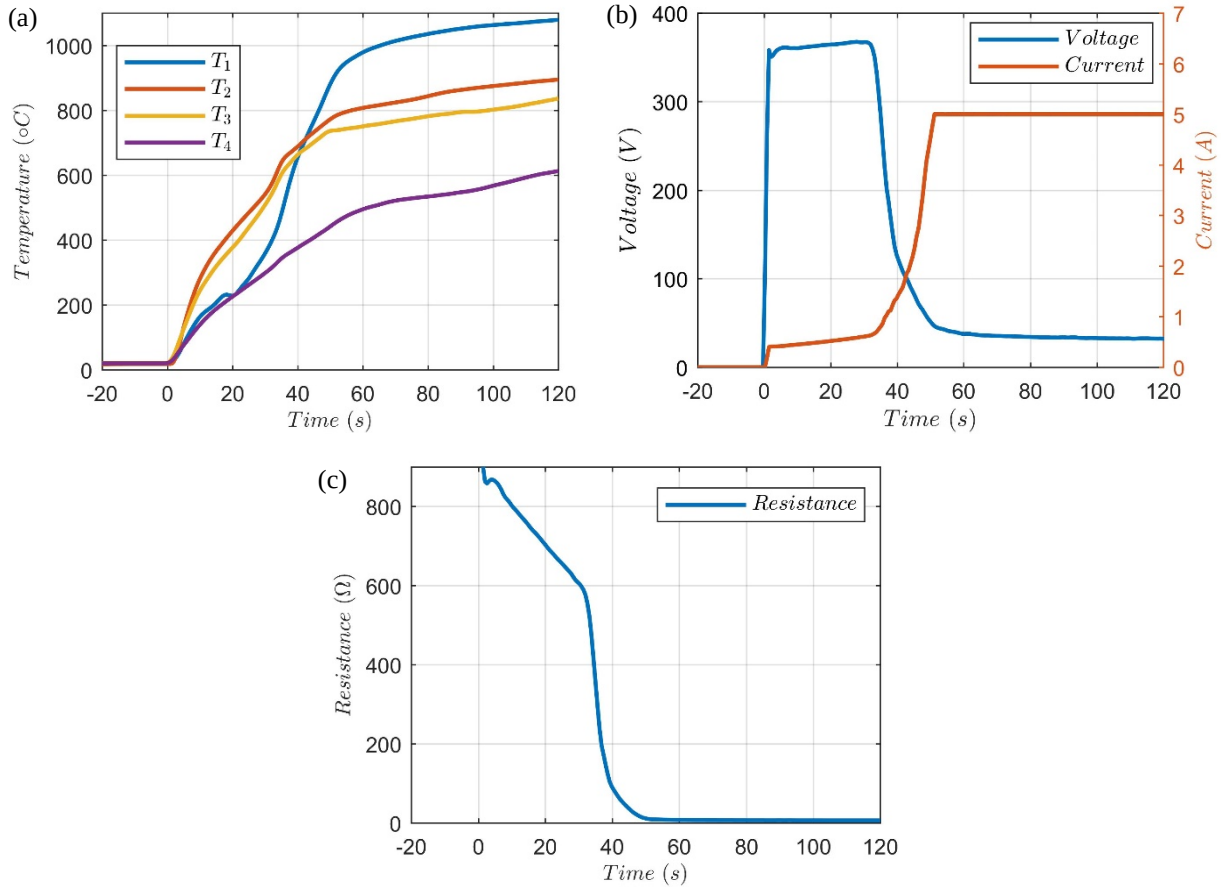

Figure 9. Ignition characteristics, 2nd configuration, $\dot{m}$ =1.75 sccm, (a) thermal profile, (b), voltage-current profile (c) resistance profile

Thus from cold after around 50 seconds the keeper discharge is in nominal operation, compared with 7-10 minutes for conventional ohmic heated cathodes[8]. Although once nominal operation is reached the discharge is not directly in thermal steady state operation, as it can take over 30 minutes for reasonable thermal equilibrium to be reached. During the thermal equilibrium there is a small voltage drop, around 5 V, and the greatest temperature change is in T_4 and smallest in T_1. Once the process of establishing nominal operation of the keeper discharge is reached an anode discharge can then be formed by applying a potential to an anode downstream, though this configuration has not been tested in this study, and keeper orifice enlargement is almost certainly required for such operation, due to the poor electron optics of the current 0.25 mm orifice.

In Figure 9, it can also be seen that T_2 and T_3 raises to ~1.7 times T_1 and T_4 for the first 25 seconds indicating that the resultant heat flux to the emitter surface raises the temperature at the center of the emitter during the initial heating phase, with edges of the emitter remaining coldest. The emitter tip, T_1 begins to diverge from T_4 at 25 seconds, ~10 seconds prior to V-I indication of transition occurring. This indicates the discharge location begins a transition to the emitter tip even with the absence of the production of significant thermionic emission. Though it may be that emitter tip edge heats significantly to thermionically emit, despite the bulk emitter being relatively cold.

At the transition range 35-50 seconds, there is a sharp increase in T_1 at a rate of 27°C/s, this combined with the sudden drop in the voltage from 366 to 50 V, as the current rises to the 5 A set point, indicates a combined transition of the electron production from primarily secondary election emission to primarily thermionic emission as well as movement of the discharge attachment from the emitter center/whole to the emitter tip. After 50 seconds to 120 seconds shown, the rate of temperature increase reduces by an order of magnitude, for T_1 to only 3°C/s, which is due to transitioning toward thermal equilibrium. During the 70 second time period of nominal operation shown, where the current is 5 A, the voltage reduces from 51 to 31 V, further reduction is noticed over 30 minutes to 25 V.

The resistance gradually drops from 900 ohms to 600 ohms after the breakdown, until the transition where there is a rapid drop to 10 ohms at nominal operation and after the full 2 minutes shown in the plot, the resistances levels off to 6 ohms.

C. Enclosed keeper – steady state operation

Figure 10 shows the typical operating characteristics from 5 to 8 A, at 1.75 sccm. As the current increase the peak emitter temperature remains at the tip T_1 with an almost linear increase of 16°C/A. T_2 to T_4 all increase through the current range, maintaining a similar profile throughout. The voltage at 5 A is 24.5 V and decreases to 19.2 V at 8 A, the power respectively is 123 W to 154 W at 8 A. This profile can be seen to be similar to that of the external configuration results (see Figure 8), such that the external configuration is reasonable simulation of the enclosed configuration for investigation of the discharge phenomenon's.

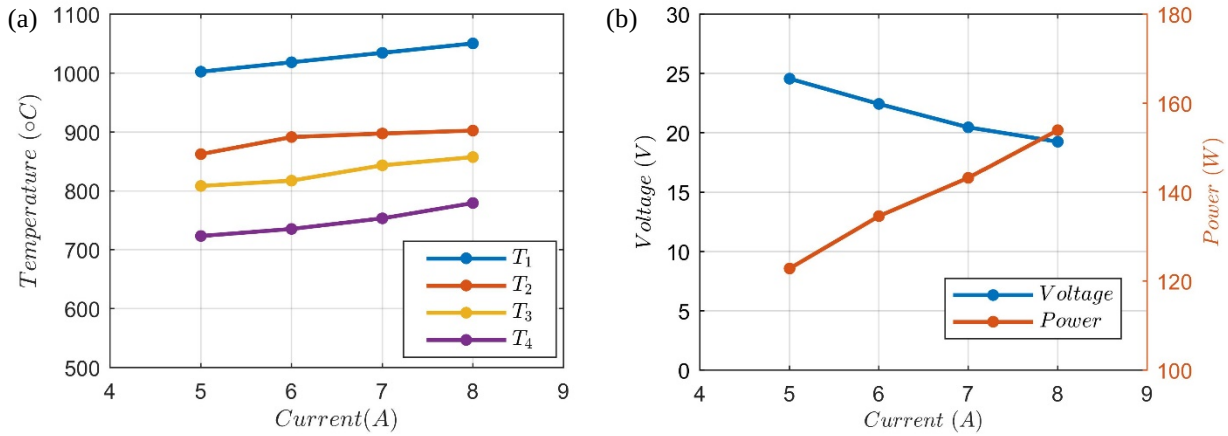

Figure 10. Operational characteristics, $\dot{m}$ =1.75 sccm, 2nd configuration, (a) temperature vs. current (b) voltage & power vs. current

D. Enclosed keeper – mass flow dependence

In Figure 11, the mass flow rate to temperature profile can be seen for a 5 A discharge. Note that T_2 and T_3 became disconnected from the emitter during this test, and hence is not plotted. The HHC operated stably from 1.75 sccm down to a mere 0.2 sccm, which was the lowest possible non-closed set point for the mass flow rate controller used in this experimental campaign. The insert temperature was seen to increase with decreasing flow rate, the emitter tip T_1 increased in centigrade by 13% and the rear of the emitter raises by over 40%, signifying the discharge starting to transition further upstream of the cathode. Similar behavior of heating of the upstream side of the emitter with lower flow rates has been reported in conventionally ignited LaB_6[8].

The cathode line pressure which is measured ~10 cm upstream from the cathode emitter displays the pressure change with flow rate before ignition and after ignition, in steady state mode. It can be seen that the pressure in the cathode line greatly increases in nominal operation, by a factor of around 1.6.

Figure 12 shows the operation of the heaterless hollow cathode in enclosed configuration at 1.75 sccm, 2 A. There is no anode present during this test, but the flow of the plasma through the orifice is apparent.

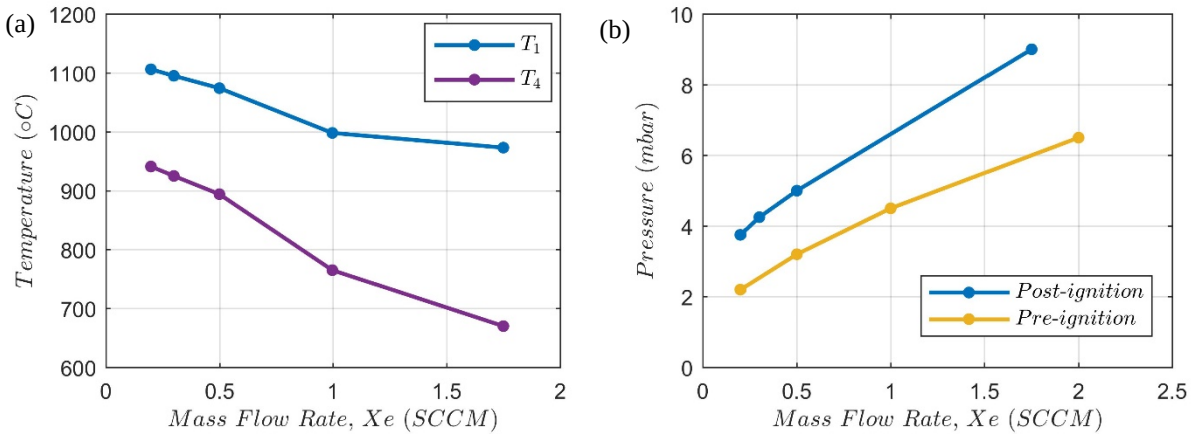

Figure 11. Flow profile, 2nd configuration, $I_k = 5$ A, (a) temperature vs. mass flow rate (b) voltage & power vs. mass flow rate

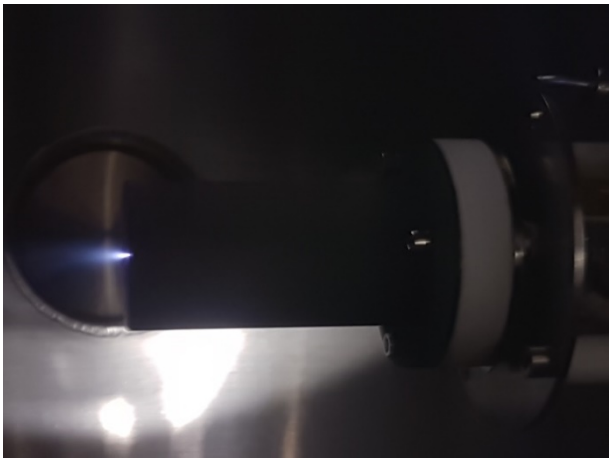

Figure 12. HHC Keeper only discharge, 2nd configuration, $\dot{m}$ =1.75 sccm, I_k =2 A

IV.Instrumentation considerations

The thermocouple instrumentation was found to reasonably represent the profile trend of the emitter temperature, though work is needed due to two issues uncounted with the instrumentation:

(a) Reliability issues, it was found that during sustained operation, occasional one or two of the thermocouples did encounter large sudden drops in temperature, with all other parameters/diagnostics measurements remaining constant. This reliability issue was attributed to poor thermal contact, such as the thermocouple detecting from the emitter due to the thermal expansion of the cathode tube or perhaps material interactions such as carbon and boron diffusion into the tungsten-rhenium thermocouples. Re-attachments of the thermocouples where performed, which did improve the reliability, the trends where the very similar after re-attachment. Note that all data presented in this study was taken with no modification to the instrumentation to insure continuity of results.

(b) Absolute values of the thermocouple readings, which were found to be significantly lower than that of the pyrometer measurements, this was predominantly attributed to poor thermal contact resistance of the graphite sleeve and emitter.

These combined issues are intended to be solved by embedding the emitter through the emitter sleeve into the LaB_6 emitter directly, to reduce the thermal contact resistance and this will be combined with more substantial insulation over the thermocouples to maintain a contact buffer due to the discussed diffusion issues.

V.Conclusion

A modular LaB_6 heaterless hollow cathode has demonstrated stable ignition to a keeper discharge of 5 A from room temperature to over 1400°C in 10s of seconds. The cathode operated reliable up to 8 A and at 1.75 sccm and down to just 0.2 sccm at 5 A. The ignition profile has been characterized, showing the emitter to heat centrally before changing to heating predominantly at the emitter tip.

The overall steady state operating parameters both with varying current and flow of the HHC were found to be similar to that of conventional hollow cathodes. This is due the HHC once being ignited operating in the same mode as a conventional cathode. The main difference being geometric, in terms of reduced keeper orifice, which effectively acts as a cathode orifice in terms of pressure profile.

The temperatures measured from the pyrometer are found to be 200-150°C below that theoretically predicted by the Richardson equation assuming uniform attachment. This may be attributed to the schottky effect, ionic current, and surface chemistry effects, and will be further investigated.

Subsequent tests will focus on the emitter thermal characteristics with an anode discharge, in which the keeper office will be enlarged to enable reasonable current extraction, up to 10 A. The aim being to determine a suitable operating range in terms of the electron optics of the keeper orifice and reasonable starting conditions, i.e <20 sccm and <500 V ignition voltages. The thermal diagnostics will also provide data for thermal simulation validation, in addition to characterizing the emitter thermal behavior throughout the various operating conditions.

Acknowledgments

The authors would like to express their gratitude to the Tony Davis High voltage laboratory for their assistance in the fabrication of this heaterless hollow cathode and use of the testing facilities. In addition, the authors received generous financial support from the ImechE, which enabled this dissemination of the work.

References

[1]D. Goebel and E. Chu, "High-Current Lanthanum Hexaboride Hollow Cathode for High-Power Hall Thrusters," *Journal of Propulsion and Power,* vol. 30, pp. 35-40, 2014.

[2]M. Schatz, "Heaterless Ignition of Inert Gas Ion Thruster Hollow Cathodes," in *18th International Electric Propulsion Conference,* Alexandria, USA, September 30-October 2, 1985.

[3]A. Daykin-Iliopoulos, S. Gabriel, I. Golosnoy, K. Kubota, and I. Funaki, "Investigation of Heaterless Hollow Cathode Breakdown," in *34th International Electric Propulsion Conference,* Hyogo-Kobe, Japan, 2015.

[4]V. Vekselman, "Characterization of a Heaterless Hollow Cathode," *Journal of Propulsion and Power,* vol. 29, pp. 475-486, 2013.

[5]D. Goebel and I. Katz, "Hollow Cathodes," in *Fundamentals of Electric Propulsion: Ion and Hall Thrusters*, ed Hoboken: Willy, 2008, pp. 243-315.

[6]J. Anderson, *Fundamentals of Aerodynamics*. Boston: McGraw-Hill, 2001.

[7]Omega, "Tungsten-Rhenium Twisted Beaded Thermocouples," OMEGA, London, UK2016.

[8]J. Polk, D. Goebel, and P. Guerreo, "Thermal Characteristics of a Lanthanum Hexaboride Hollow Cathode," in *34th International Electric Propulsion Conference*, Kobe, Japan, 2015.

[9]Cotronics, "Resbond 904 Adhesive & Coating-Bonds-Coats-Protects," Cotronics Corporation, New York, USA2016.

[10]E. Storms and B. Mueller, "A Study of Surface Stoichiometry and Thermionic Emission Using Lab6," *Journal of Applied Physics*, vol. 50, pp. 3691-3698, 1979.

[11]L. Michalski, *Temperature Measurement*. Chicago: Wiley, 2001.

[12]D. Jacobson and E. Storms, "Work Function Measurement of Lanthanum-Boron Compounds," *IEEE Transactions on Plasma Science*, vol. 6, pp. 191-199, 1978.

[13]L. Favreau, "Cataphoretic Coating Lanthanum Boride on Rhenium Filaments," *Review of Scientific Instruments*, vol. 36, pp. 856-857, 1965.

[14]O. Richardson, "Electron Theory of Matter," *Cambridge Physical Series*, vol. 23, pp. 594-627, 1914.

[15]D. Goebel and E. Chu, "High Current Lanthanum Hexaboride Hollow Cathodes for High Power Hall Thrusters," in *32nd International Electric Propulsion Conference*, Wiesbaden, Germany, 2011.